Multistatic Radar Data Fusion For Detection With Reduced Transmit Power Consumption

Dilan Dhulashia, Matthew A. Ritchie*
Department of Electronic and Electrical Engineering
University College London
London, U.K.
{dilan.dhulashia.15}{m.ritchie}*@ucl.ac.uk

***Abstract*—This paper presents a quantitative comparison of the detection performance of two multistatic radar detection methods; the first limited by a communications constraint between its constituent nodes and the second with unlimited communications capacity. The methods are tested for a selection of scenarios with differing target positions, and the transmit power requirements to obtain a similar level of detection performance to that of a monostatic radar are analysed. The scenarios simulated are in two-dimensional space and the multistatic system considered is comprised of a single transmit and three distributed receive nodes. A cell-averaging constant false alarm rate is used for the monostatic and both multistatic detection methodologies proposed. It is found that data fusion at a lower level of abstraction, where communications are non-constrained, can lead to better detection performance in multistatic systems. Additionally, the power resource savings compared to an equivalent performance monostatic system are also presented as part of this work.**

***Index Terms*—Detection, Multistatic Radar, Data Fusion, Power Consumption**

I. Introduction

Distributed multistatic systems have attracted significant attention from the radar community in recent years due to the potential benefits they offer over conventional radar systems for the performance of multiple traditional radar modalities, including: detection, parameter state estimation, and tracking. Networked radar systems are posited to offer improved performance for equivalent resource consumption, while additionally offering logistical benefits, for example, graceful degradation, covertness, and hybrid operation [1], [2]. However, the successful operation of a multistatic radar system comes with added complexity over its traditional counterparts. Achieving coherency between the nodes requires an accurate common appreciation of space and time across the system; practical realisation of these capabilities is an ongoing technical challenge. An added complexity arises from the need to operate in conditions in which communications capacity between nodes is constrained. Further to this, it remains an open problem as how to optimally process the multiple channels of multistatic radar data and make operational decisions relating to the radar modalities based on the data obtained across the entirety of the multistatic network.

Previous work has looked to study the optimisation of power resource allocation across the nodes within a multistatic system with respect to probability of detection metrics [3], as well as to consider distributed sensing systems where separated node clusters are incapable of communication, with the goal of minimising transmission power usage [4].

In [5], a geometry based formulation for detection with multistatic systems is proposed which utilises the association of points in a range-Doppler space to a linear subspace consisting of appropriately time and Doppler shifted variants of the transmitted waveform. This research provides a framework within which radar data quality may be understood as a function of multistatic geometry and signal characteristics.

Research reported in [6] looked to move beyond the detection problem by studying parameter state estimate accuracy achievable by multistatic systems using a centralised data fusion technique made possible through a priori knowledge of a fixed system geometry.

A thorough overview of the literature addressing detection in multistatic radar systems is provided in [7], including examples of non-coherent and coherent synchronisation techniques. The authors examine a coherent multistatic system and propose a centralised joint spatial processing technique which considers the synchronisation requirements in space, time, phase and frequency. The system size, in terms of node quantity and geometry required for ambiguity elimination, is presented.

This paper aims to investigate two methodologies for fusing multistatic radar data at two different levels of abstraction and novelly compares the required power consumption by each in order to achieve similar levels of performance to a monostatic alternative, when system characteristics are equivalently specified and a signal level modelling approach is used. A Monte-Carlo approach is used to produce statistical measures of traditional probabilistic radar performance metrics.

The rest of the paper is organised as follows: The simulation model and a description of the radar received signals is given in Section II. In Section III, the target detection problem is formalised and the approaches used by the different system architectures studied in this paper are provided. Section IV provides information regarding the test scenarios used in the investigations simulated and the results from the simulations are given in Section V. Finally, Section VI concludes the findings of the paper.

This work was supported by Thales UK and the Engineering and Physical Sciences Research Council (EPSRC) under grant number: EP/R513143/1

II. Simulation Model

A. Signal Model

A multistatic radar simulator, capable of modelling the digitised baseband radar signals at each node, was developed as part of this research and was used to carry out the simulations used in this work. The representation of the baseband signal obtained at a radar receiver's (Rx) surveillance channel prior to implementation of the correlation procedure (i.e. the signal immediately following analog-to-digital conversion (ADC)), can be considered as a delayed copy of the waveform radiated from the transmitter (Tx) which has undergone an amplitude scaling due to path loss effects and reflection from a target, as well as phase and frequency shifts due to the delay and the target relative velocity, respectively. The received signals are embedded within noise due to the Rx characteristics, and other non-deterministic terms may also be present. The digitised received signal at a discrete time sample t is then a stochastic variable described formally as:

$$r[t] = s[t - \hat{\tau}]\sqrt{PL\sigma}e^{j2\pi(f_D t + f_c \hat{\tau})} + n[t], \tag{1}$$

where s is the baseband transmitted waveform with normalised amplitude, P is the transmit power used, L is a loss term encompassing all losses incurred along the transmission path from Tx to Rx [8], σ is the target radar cross-section (RCS), f_D is the Doppler frequency shift due to relative motion between the target at the radar nodes, f_c is the carrier frequency used, $\hat{\tau}$ denotes the closest integer number of intra-pulse (fast-time) samples corresponding to τ, the exact delay between signal transmission and reflection reception, and $n[t]$ is the stochastic noise signal which is assumed to be purely additive.

The signals received at each Rx within the multistatic radar system can be considered simultaneously by adopting the matrix notation such that the received data is treated as a matrix with rows corresponding to individual Rx's and where each column represents a discrete time sample. In such a case, the terms P, L, σ, τ and f_D in (1) must all become vectors with elements corresponding to the appropriate value for a particular Rx within the system. In such a case, $n[t]$ becomes a matrix of similar dimensions to that representing the received data, since it must be assumed that the noise at each Rx site is independent. The research in this paper is concerned with the single Tx, multiple Rx type network, where only a single target is present. As such, it is sufficient to consider only the single transmitted signal at each Rx. If multiple Tx were present, the terms within the signal model must become vectors with elements defining characteristics between each Tx-Rx pair, as each surveillance signal at each Rx would be a superposition of reflections from the target. It should also be noted that, in all cases, terms σ and f_D are geometry dependent.

The multistatic radar system can architecturally be considered to be comprised of a set of bistatic radar pairs. Therefore, each Rx node in the system also requires a reference channel in order to obtain a copy of the transmitted waveform along a direct-path, from Tx to Rx. A single, one-dimensional correlation operation between the reference channel signal and the surveillance channel signal is performed in order to generate a typical bistatic-range profile from the received signals. The monostatic radar correlation process can be considered as a special case of this, where the reference signal is substituted for a lossless copy of the normalised baseband Tx waveform. In the monostatic case, the delay corresponds to a two-way range as opposed to a bistatic range, as in the case of each Tx-Rx pair within the multistatic radar system.

Direct-Path-Interference (DPI) suppression must be performed on the resultant correlated signal at Rx nodes in the multistatic system in order to reduce contribution within the surveillance signal arising from the transmitted signal which enters the surveillance Rx following a direct path trajectory (i.e. without having undergone reflection). In both the monostatic case, and for each Rx in the multistatic case, it is possible to then integrate across the range-profiles corresponding to the reception of each pulse within the CPI, to produce an integrated profile (IP).

In this work, the target was assumed to possess similar radar cross-section (RCS) characteristics to that of a small quadcopter style drone. The target RCS is approximated using a method designed in order to capture the effects of both the bistatic angle within the geometry formed by the Tx, Rx, and target nodes, as well as the aspect angle between the target and the line-of-sight from the Tx node and the target. This is achieved using the following RCS model:

$$\sigma\left(\theta, \varphi, f_c\right) = A\left(\theta, f_c\right) B\left(\varphi, f_c\right), \tag{2}$$

where $A\left(\theta, f_c\right)$ is the bistatic RCS of a perfect electric conductor (PEC) sphere of one meter diameter at a bistatic angle of θ, analysed using incident radiation of frequency f_c and limited to the azimuth plane, and $B\left(\varphi, f_c\right)$ is the monostatic RCS of a small-quadcopter drone model observed from an aspect angle φ and irradiated with radiation of frequency f_c. The analysis frequency, f_c, takes the same value as that used for the Tx waveform carrier frequency in subsequent parts of this paper.

The additive noise signal used to model the statistical Rx noise process is denoted $n[t]$ in (1). The noise signal is considered to be comprised of discrete complex noise samples. Each sample contains a real and imaginary component, where each of these is considered an independent Gaussian random variable with a mean value of zero and a variance proportional to half of the total power of the Rx noise. The Rx noise power is well understood to be a function of temperature, Rx bandwidth, and other characteristics intrinsic to the Rx node. Physical phenomena which lead to additional stochasticity beyond thermal noise effects (for example, drone blade-flash contributions to the target RCS) were not modelled in this work.

B. Transmitter and Receiver Structure

The Tx and Rx nodes modelled in the simulations are assumed to have isotropic directionality. In the case of the

Rxs, it is assumed that, while each Rx is capable of receiving radiation from all directions, it is also capable of distinguishing the direction-of-arrival (DOA) of a given reflection with perfect precision. Therefore, it is assumed that each Rx node can locally compute a separate IP for all directions, simultaneously (i.e. N_{DOA} IPs will be recorded at each Rx), and that the signal reflected from a target is constrained to only be present at a single direction from the Rx (i.e. no sidelobes are present). As $N_{DOA} \rightarrow \infty$, the capability for spatial correlation consensus between the different Rx nodes becomes exactly precise for any location within the scenario region of interest. While these assumptions rely on a Rx model which is theoretical due to both pragmatic and fundamental limitations, they do provide a framework within which the optimal detection performance achievable by the methodologies tested may be analysed for a given set of operating characteristics and problem parameters. The results can therefore be considered an empirically achieved quantitative reflection of the upper bound on the system performance.

III. Detection Problem

The target detection problem refers to the process of determining whether or not a target should be considered to be present within a given sample of the radar data [9]. Consider a single received radar pulse due to a reflection of the transmitted signal off a target located at a range corresponding to the time delay, τ, which has been sampled at a rate such that the signal is represented by I complex samples occurring at discrete points in time. The determination of whether or not a target is present at a specific range, that is, whether or not it should be determined that a target is present in the discrete sample bin, i, where $i \in [1, I]$, can then be formalised by considering the observed signal value and formulating the following hypothesis test:

$$\begin{aligned} H_0 &: r\left[i\right] = n\left[i\right], \\ H_1 &: r\left[i\right] = s[i-\hat{\tau}]\sqrt{PL\sigma}e^{j2\pi(f_D i + f_c \hat{\tau})} + n[i], \end{aligned} \tag{3}$$

where H_0 and H_1 correspond to the target being absent and present, respectively. $\hat{\tau}$ is again used to denote the closest integer number of samples corresponding to the delay time.

Using the two hypotheses conditions defined in (3) and a statistical model which is assumed to underlie the stochasticity, it is possible to define probability density functions for the observed received signal value conditional on either of the hypotheses having occurred. An optimal form of the detection process is then based on the likelihood ratio test which can be formulated based on the conditional probability density functions of a given observation having been made with respect to each hypothesis. A comprehensive derivation of this can be found in [10].

In the work presented in this paper, three detection methods are used. Each method utilises a similar approach to determine a dynamic threshold value, namely, an implementation of a cell-averaging constant false alarm rate (CFAR) type detection algorithm; however, the abstraction level at which the observed data and decisions are made vary. The first method is for use by the monostatic system and attempts detection on matched filtered radar data.

The second method is referred to as the 'Limited Communications' technique is for use by the multistatic system. This method attempts local detection at each Rx node before making a centralised, global detection decision based on the local votes.

The final detection method is referred to as the 'Unlimited Communications' method and is also for use by the multistatic system. This method aims to provide low-level data fusion between the different Rxs by collecting and joining IP signal data from each node prior to attempting detection on the joint data. Since the CFAR algorithm forms the basis of all three detection methods used, it is appropriate to first describe how this technique works before describing the detection methods.

A. Constant False Alarm Rate Algorithm

Consider an IP obtained by a monostatic radar. The range observed is the two-way range, while in the case of a Rx within a bistatic pair, the range observed is the difference between the bistatic range and the baseline length between the Tx and Rx nodes which form the pair. The samples within an IP correspond to the discrete samples in time (equivalently range-bins).

The CFAR technique can be applied to the IP by considering each time sample within the profile sequentially. For each sample, known as a cell-under-test (CUT), within the profile, the following test is performed:

$$|r[i]| \underset{<H_0}{\geq H_1} q_t \left(\rho_{fa}^{\frac{-1}{q_t}} - 1 \right) \frac{\sum_{k=i-q_s}^{i-\frac{q_g}{2}} |r[k]| + \sum_{k=i+\frac{q_g}{2}}^{i+q_s} |r[k]|}{q_t} \tag{4}$$

where $r[i]$ is the observed value of the IP in the i^{th} bin under test, q_t and q_g are constants defining the total number of test cells and guard cells, respectively, q_s is half the sum of q_t and q_g, and ρ_{fa} is the desired rate of false alarm occurrences. The right-hand side of (4) forms a threshold for the CUT. If the value of the CUT exceeds the threshold, a target is deemed to be detected, while if the threshold is not exceeded, a target is assumed to be absent. The values used for q_t and q_g are unchanged regardless of which of the methods defined in Sections III-B, III-C, or III-D is utilising the CFAR technique. The values selected for these parameters were chosen and verified via empirical testing and are $q_t = 100$ and $q_g = 2000$.

B. Monostatic Detection

In this detection method, the CFAR technique is applied exactly as described in Section III-A to a single IP, corresponding to that obtained from the DOA the reflection from the target is obtained at. The false alarm rate is set to be 1×10^{-6}. It should be noted that, in accordance with the assumptions laid out in Section II-B, the monostatic system generates N_{DOA} IPs; however, only a single IP corresponds to the direction in

which the target is present. As such, it is only necessary to simulate and consider this IP. Any IP arising from other DOAs would only contribute to the number of false alarms which are registered and would have no influence on the number of detections or misses which occur.

Given this IP is selected, the indexes of each CUT at which a detection is deemed to have occurred is recorded. In order to determine the number of: true detections, misses, and false alarms, the recorded indexes are compared to the known true index in which the target lies. An allowable inclusion zone is configured to surround the true target index, such that any detections which occur within cells in this zone are permitted to be counted as a true detection. The number of cells which form the inclusion zone is chosen to be two (i.e. one cell either side of the true cell). This corresponds to an inclusion zone size of 1.8 m, based on the sampling rate used (see Table. II). The number of true detections and misses are considered as mutually exclusive choices. That is, as long as at least one detection is made within the inclusion zone, a true detection is said to have been made. If no detections are made in the inclusion zone, a miss is said to have occurred.

The total number of detections made outside of a zone defined as surrounding the true target cell by half the radar range resolution on either side, is determined to be the number of false alarms. This variable can take any value (up to the total number of cells excluding the size of the inclusion zone), and is therefore not limited to the binary choice.

C. Multistatic Detection: Limited Communications

This method aims to consider how a multistatic radar system may leverage its multiple Rx nodes in order to aid detection capabilities while there exists a limitation on the amount of data which can be shared across its nodes. This represents data fusion occurring at a high level of abstraction (i.e. after stages of processing and analysis have already occurred on the radar data). It is assumed that due to this limitation, a detection decision must be made locally at each Rx within the system, and a global decision is made based only on considerations of the local decisions.

At each local Rx site, the same procedure used as described in the monostatic detection method in Section III-B is employed. The false alarm rate at each local CFAR process is chosen to remain at 1×10^{-6}. While it may initially appear counter-intuitive to set the false alarm rate to the same value as that used in the monostatic detection method (since there are now three individual IPs contributing to each detection decision), it should be noted that, at any given triad of corresponding samples from the three individual contributing IPs which does not correspond to the true target cell, the signal information can be assumed to be entirely uncorrelated. [1] This is equivalent to the fact that the only point of spatial correlation between the three IPs obtained is the sample at which the target is located. Samples preceding or subsequent to this cell in each of the IPs would correspond to differing positions in space and the signal within these samples can therefore be assumed to be independent.

It should further be noted that, under the assumptions made in Section II-B, across the system there would be a total of $N_{Rx}N_{DOA}$ IPs recorded; however, it is only necessary to consider the single IP at each Rx corresponding to the specific direction in which the target is positioned relative to that Rx. Each Rx within the system is then only required to share the indexes of the CUT at which it registered a detection. In order to measure the detection performance of the system, the indexes recorded by each Rx are compared with the true cell, relative to each Rx, at which the target is known to be. In each case, the same inclusion zone limits as defined in the monostatic detection tests are employed.

A global decision can then be considered by an aggregated vote across the Rxs. That is, if a triad of detections across all Rxs can be formed by taking a single detection from each Rx, and these detections corroborate each other (i.e. can create bistatic ellipses which intersect at a unique location), the multistatic system is deemed to have made a detection overall. A false alarm from the multistatic system is defined to occur only when all three Rxs register a detection outside of their respective inclusion zones which occur at indexes which corroborate one another but no target exists there. This determination is possible only under the assumption that the relative positions of the radar nodes is known and the Rx model described in Section II-B is utilised. It should be noted that, in two-dimensional space, if more Rx nodes were used, the final decision making procedure still only requires agreement across at least three nodes.

D. Multistatic Detection: Unlimited Communications

This method aims to consider how a multistatic radar system may perform detection given no constraints on the systems communications capabilities. This represents data fusion occurring at a lower level of abstraction (i.e. at a level closer to raw radar signal data). It is therefore assumed that data may be shared between the Rxs in the system at a IP level. That is, N_{DOA} IPs containing complex valued data may be generated at each Rx site and shared to a centralised computation point. Each IP from each Rx node must be appropriately superimposed combinatorially with IPs from the other Rxs, such that a final total of $(N_{DOA})^{N_{Rx}}$ multistatic-IPs (MIP) are obtained. For each MIP, the different contributions from each Rx node must be adjusted to account for relative positioning of the Rx nodes within the system prior to the superposition process. Analogous to the methodological procedures described in Section III-B and III-C, it is assumed to be sufficient to simulate the data pertaining only to the MIP in which the target is present. The adjustment procedure prior to superimposing the individual contributing IPs requires that the distance between each Rx and every point within a region of interest within which the detection problem is geographically constrained be known.

[1] During simulations, it was observed that the intermediary probability of false alarms occurring at each local decision maker corresponded with the set false alarm rate. The overall global decision maker consistently produces a probability of false alarm several orders of magnitude lower than this.

The CFAR technique can be used as described in Section III-A on the single MIP generated with the false alarm rate set to 1×10^{-6}. The recording of true detections, misses, and false alarms can then be carried out in a similar manner to the monostatic detection case.

IV. Test Scenarios

Testing of the detection methods described requires the simulation of a monostatic and a multistatic radar system, each attempting to use the techniques to detect a target positioned at a selection of test positions. A monostatic system and a single Tx, triple Rx multistatic system are therefore considered, and the positions of the Tx, Rx, and target entities used in the simulated scenarios are depicted in Fig. 1.

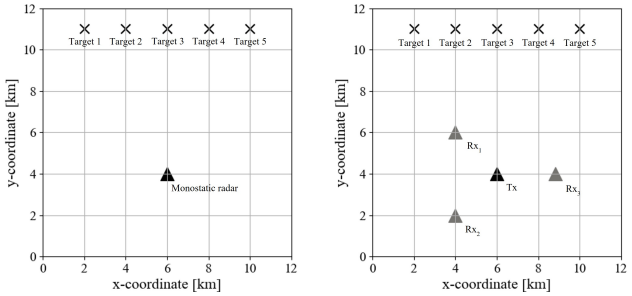

Fig. 1: Maps showing relative positions of entities used in simulated scenarios: (a) Monostatic radar (B) Multistatic radar

It should be noted, while simulations are carried out for five target positions, only one target is ever present in a given simulation. The target aspect angle is chosen such that it is orientated to always face the positive x-direction. The Rx positions in the multistatic system are chosen such that they are equidistant from the position at which the monostatic system was placed. The full characteristics used for the Tx waveform and the Rx nodes are provided in Table. I and II, respectively.

TABLE I: Transmit Waveform Parameters

Parameter	Monostatic	Multistatic
Tx power [kW]	5	3-6
Type	Rectangular	Rectangular
Carrier frequency [GHz]	1	1
Duty cycle [%]	1	1
PRF [Hz]	5000	5000
CPI [pulses]	8	8

TABLE II: Receiver Node Operating Characteristics

Parameter	Value
Gain [dBi]	9
Frequency band [GHz]	0.9-1.1
Sampling frequency [MHz]	500
Noise figure [dB]	8
DPI suppression [dB]	150

In order to obtain empirical measures of the detection performance, a Monte-Carlo simulation approach is used. For a given target position and radar system configuration, 10,000 repetitions of the detection problem are simulated. In each repetition of the simulation of the monostatic detection problem scenario, the detection methodology described in Section III-B is applied to the generated data. Similarly, for each repetition of the multistatic detection problem scenario, both detection methodologies described in Sections III-C and III-D are applied to the generated data. The results reported are presented as they pertain to each of the five target positions tested. For each detection methodology and target position pairing, the detection performance is calculated as aggregated scores from the repetitions carried out for that pairing and the observations of detections and false alarms made.

V. Simulation Results

The probability of detection as a function of the Tx power, for each of the multistatic radar detection methodologies, are presented as graphs within Fig. 2 for each target position. In each graph, the corresponding detection performance exhibited by the monostatic radar system when using a Tx power of 5 kW is also shown, such that the equivalent Tx power required by the multistatic system to obtain a similar level of detection performance using both multistatic detection methodologies can be seen.

The results presented in Fig. 2 show that superior detection performance is achieved by the multistatic system using the 'Unlimited Communications' detection method, across all Tx powers and in each target position case. These results are summarised in Fig. 3 which shows the relative Tx power required by the multistatic radar system in order to reach the same detection performance level as the monostatic radar for each target position. Results for each of the proposed multistatic detection methods is shown.

The results shown in Fig. 3 indicate that a multistatic system, utilising data fusion at a low-level of abstraction, will require significantly less Tx power to achieve an equivalent detection performance to a monostatic system. However, this is only partially true for a multistatic system employing the 'Limited Communications' decision methodology, since two out of the five target positions show greater Tx power being required than compared to the monostatic system. In instances where this detection method is used, the results indicate that the geometry of the system relative to the target has a greater influence on whether the system offers a reduced Tx power benefit over the monostatic system.

Greater differences in the Tx power required by multistatic systems using the two multistatic detection methods are exhibited when the target is positioned closer to the more populated side of the Rx node grouping (i.e. on the left side of the scenario map), further highlighting the influence of preferential geometries within multistatic systems.

The results obtained show that the detection performance of a multistatic system utilising a low-level data fusion technique is superior in all tested cases compared to an equivalent system utilising a high-level data fusion technique.

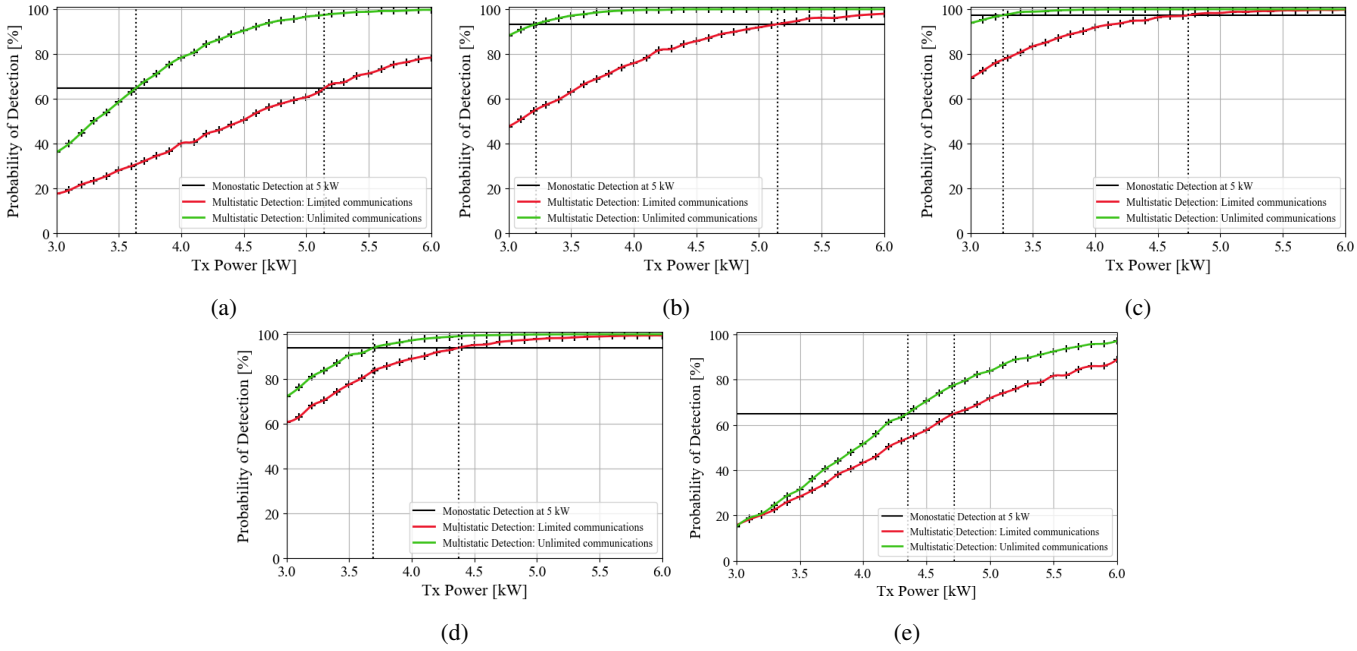

Fig. 2: Probability of detection from target position: (a) Target 1 (b) Target 2 (c) Target 3 (d) Target 4 (e) Target 5

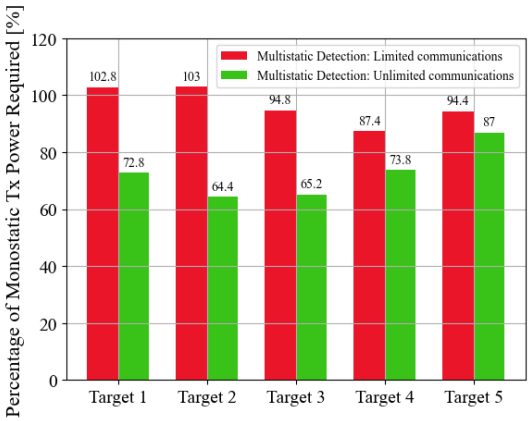

Fig. 3: Proportion of monostatic Tx power necessary to obtain similar probability of detection with multistatic radar

VI. Conclusion

In this work, the relative power resources required to obtain the same level of detection performance in a multistatic radar system using two detection methods were compared. The detection performance of a monostatic system was included as a comparative baseline. It was shown quantitatively via Monte-Carlo simulation that a multistatic radar system performing detection based on radar data fused at a low-level of abstraction is capable of achieving the same level of detection performance, while using lower power consumption, compared to an equivalent system which requires locally made detections prior to a voting process. To realise the full potential of a multistatic radar system's detection capabilities, data sharing between nodes and fusion at a point closer to the raw radar signal data is preferable.

References

[1] V. S. Chernyak, Fundamentals of Multisite Radar Systems. Multistatic Radars and Multiradar Systems, Amsterdam: Gordon and Breach Science Publishers, 1998.

[2] D. Dhulashia, M. Temiz, and M. A. Ritchie, "Jamming Effects on Hybrid Multistatic Radar Network Range and Velocity Estimation Errors," IEEE Access, 10, 2022, 27736-27749.

[3] T. Aittomäki, H. Godrich, H. V. Poor and V. Koivunen, "Resource allocation for target detection in distributed MIMO radars," 2011 Conference Record of the Forty Fifth Asilomar Conference on Signals, Systems and Computers (ASILOMAR), pp. 873-877, 2011, doi: 10.1109/ACSSC.2011.6190133.

[4] A. Deligiannis, A. Panoui, S. Lambotharan and J. A. Chambers, "Game-Theoretic Power Allocation and the Nash Equilibrium Analysis for a Multistatic MIMO Radar Network," in IEEE Transactions on Signal Processing, vol. 65, no. 24, pp. 6397-6408, 15 Dec.15, 2017, doi: 10.1109/TSP.2017.2755591.

[5] S. D. Howard, S. Sirianunpiboon and D. Cochran, "A Geometric View of Multistatic Radar Detection," 2018 52nd Asilomar Conference on Signals, Systems, and Computers, pp. 911-915, 2018, doi: 10.1109/ACSSC.2018.8645202.

[6] P. Stinco, M. Greco and F. Gini, "Data fusion in a multistatic radar system," Proceedings of the Institute of Acoustics, 32, pp. 146-151, 2010.

[7] P. E. Berry, N. Dahal and K. Venkataraman, "On the design of an optimal coherent multistatic radar network configuration," IET Radar Sonar Navig. 16(5), pp. 869–884, 2022, https://doi.org/10.1049/rsn2.12226.

[8] M. Skolnik, Introduction to Radar Systems, 3rd ed., Columbus, OH: McGraw-Hill, 2001.

[9] H. L. Van Trees, Detection, Estimation and Modulation Theory, vol. III. Hoboken, NJ: Wiley, 1971.

[10] S. Jebali, H. Keshavarz, and M. Allahdadi, "Joint Power allocation and target detection in distributed MIMO radars," IET Radar, Sonar & Navigation, vol. 15(11), pp. 1433-1447, November 2021.